Accurate Lever Arm Determination via 3D Triangulation for Aided Inertial Navigation Systems

(Destekli Ataletsel Navigasyon Sistemlerinde 3B Üçgenleme Yöntemi ile Kol Kaçıklığının Hassas Olarak Belirlenmesi)

Mehmet SİMAV*, Yunus Aytaç AKDOĞAN
Harita Genel Müdürlüğü, Ankara
*Sorumlu yazar: mehmet.simav@harita.gov.tr

Received (Geliş Tarihi): 15.05.2022 Accepted (Kabul Tarihi): 27.07.2022

ABSTRACT

It is a well-known fact that the utilization of erroneous lever arm values in an aided inertial navigation system degrades the accuracy of the navigation solution. In practice, lever arm determination can be difficult, in particular when the displacement between the aiding sensors such as GNSS antenna, odometer, or a laser scanner and IMU is relatively large or the line of sight between them is blocked by the vehicle chassis. This paper considers the accurate determination of lever arm vector via 3D triangulation, describes the methodology, and provides a MATLAB function for a quick implementation. Slant distance, horizontal direction, and zenith angle measurements of a total station along with the fixed positions of the reference points on the IMU casing in an experimental setup are used to estimate the aiding sensor position in the inertial sensor coordinate frame by non-linear weighted least squares adjustment. The results reveal that lever arm accuracy of a few millimeters can be achieved with a total station of a medium quality.

***Keywords**: Aided inertial navigation, lever arm vector, 3D triangulation, non-linear weighted least squares.*

ÖZ

Destekli ataletsel navigasyon sistemlerinde hatalı kol kaçıklığı değeri kullanımının, navigasyon sonuçları doğruluğunu düşürdüğü iyi bilinen bir gerçektir. Özellikle GNSS anteni, odometre veya lazer tarayıcı gibi destek sensörleri ile IMU arasındaki mesafenin göreceli olarak fazla olması veya birbirleri arasındaki görüş hattının araç gövdesi tarafından bloke edilmesi durumunda, pratikte kol kaçıklığı belirlemek zor bir durum haline gelebilir. Bu çalışma; kol kaçıklığı vektörünün 3B üçgenleme ile hassas bir şekilde belirlenmesini konu almakta, metodolojiyi tanımlamakta ve hızlı bir uygulama için bir MATLAB fonksiyonu sunmaktadır. Deneysel bir kurulum yapılarak bir total station ile elde edilen eğik mesafe, yatay doğrultu ve zenit açı ölçümleri ile birlikte IMU kasası üzerindeki referans noktalarının sabit konumları kullanılarak, destek sensörünün ataletsel sensör koordinat çerçevesindeki konumu, doğrusal-olmayan ağırlıklı en küçük kareler dengelemesi ile kestirilmiştir. Sonuçlar, orta kaliteli bir total station ile birkaç milimetre doğruluğunda kol kaçıklığının belirlenebileceğini göstermektedir.

***Anahtar Kelimeler**: Destekli ataletsel navigasyon, kol kaçıklığı vektörü, 3B üçgenleme, doğrusal-olmayan ağırlıklı en küçük kareler.*

1. INTRODUCTION

The integration of Inertial Navigation System (INS) with some aiding sensors such as Global Navigation Satellite System (GNSS), odometer, magnetometer, laser scanner, camera, or a radar altimeter aims to utilize the benefits of the individual navigation sensor and to overcome their drawbacks for a continuous, high-bandwidth, and better navigation solution. Aided inertial navigation systems have been used for many years in a wide variety of applications from underwater to space. The integration architectures may vary depending on the application of the corrections to the inertial navigation solution, types of aiding sensor measurements used, and integration algorithm adapted. But, regardless of the integration approach, the lever arm vector between the aiding sensor and the Inertial Measurement Unit (IMU) of an INS must be considered while calculating the navigation solution (Jekeli, 2001; Titterton and Weston, 2004; Farrell, 2008; Groves 2013; Grewal et al., 2013). Using erroneous lever arm values or failing to compensate for its effect yields an attitude dependent error which eventually degrades the accuracy of the navigation solution (Bell, 2000; Hong et al., 2002; He and Jianye, 2002). It is obvious that the lever arm vector should be determined with accuracy at least not worse than today's GNSS positional accuracy.

In practice, it is not possible to locate the GNSS antenna, IMU, and the other aiding sensors at the same place physically. The antenna must be mounted on the outside surface of the platform to capture signals from the GNSS satellites. The odometer is mounted on a wheel of a moving vehicle. However, the IMU is usually located inside the platform or at different spots. The non-colocation of the sensors potentially yields inconsistent position estimates of IMU and aiding sensor by the amount equal to the lever arm vector, which is the relative position of the aiding

To cite this article/Atıf: Simav, M., & Akdoğan, Y.A. (2022). Accurate Lever Arm Determination via 3D Triangulation for Aided Inertial Navigation Systems. Harita Dergisi, *168*, 38-44.

sensor resolved in the inertial sensor coordinate frame (see Figure 1). When both sensors are mounted on the platform as close as possible to each other, the lever arm vector can be measured by a simple ruler or a tape measure.

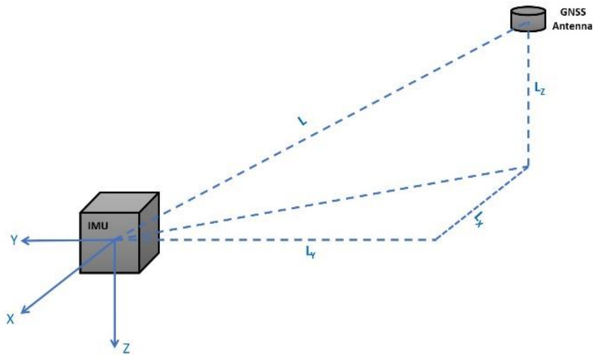

Figure 1. GNSS antenna lever arm vector resolved in the inertial sensor coordinate frame.

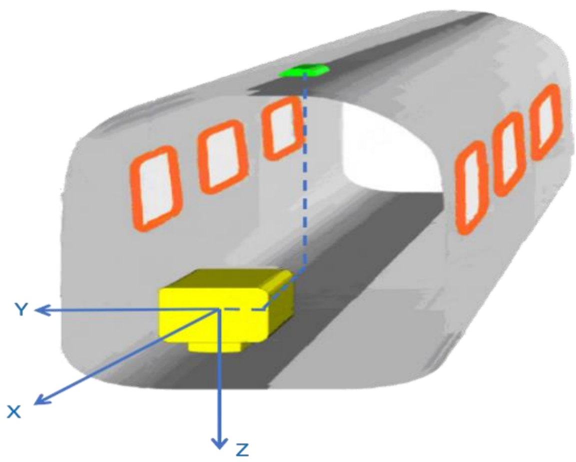

Figure 2. A typical GNSS antenna and IMU setup for the airborne applications.

But, when the displacement between the aiding sensor and IMU is relatively large or the line of sight between them is blocked by the vehicle chassis (e.g. aircraft setup in Figure 2), it is not that easy to accurately measure the components of the lever arm vector. More advanced techniques such as close-range photogrammetry (Luhmann et al., 2020) or geodetic techniques are required.

There are some computational methods proposed in the literature for the compensation of the lever arm effects provided that the lever arm vector or its magnitude is known to some accuracy level (Hong et al., 2004; Hong et al., 2005; Lee et al., 2005; Hong et al., 2006; Seo et al., 2006; Wu et al., 2014; Montalbano and Humphreys, 2018; Borko et al., 2018; Stovner and Johansen, 2019). However, all these methods increase the complexity in the computation, but it is obvious that the more accurately the lever arm is determined, the better the navigation solution is obtained. The paper considers the accurate determination of the aiding sensor lever arm vector via 3D triangulation. To the best of the author's knowledge, there exists no direct and rigorous publication about the topic that may help the non-geodesists working in the inertial navigation field. This study provides a comprehensive guide especially to novice researchers with a basic set of equations and terms for the implementation.

The 3D triangulation technique has been applied for many years particularly before the advent of satellite positioning to compute the precise coordinates of the geodetic network or control points (Torge, 2001; Awange and Grafarend, 2005). It is still in use in some local land surveying applications. The principal of the 3D triangulation is based on measuring slant distances, horizontal directions, and the vertical (zenith) angles to some reference points whose coordinates are known in an arbitrary cartesian coordinate frame (see Figure 3). The unknown coordinates of the standing and the other survey points are determined using the trigonometric relations between the observations and the point coordinates as described in Section 2. This paper is organized as follows: In Section 2 the methodology is explained and the problem is formulated mathematically. Section 3 describes the experimental setup and the measurements performed. The last part presents the results and conclusion. A MATLAB function is provided in the appendix.

2. METHODOLOGY

The method of least squares adjustment of indirect observations is employed to obtain the best estimate of the aiding sensor coordinates in the inertial sensor coordinate frame. This technique requires the formation of a set of observation equations and their solution (Alsadik, 2019; Ogundare, 2019). Because the equations are non-linear functions of the reference (known) and unknown point coordinates, linearization is employed using the approximate values. The process is iterative that the corrections for the unknowns are computed and approximate values are updated until the corrections become negligible.

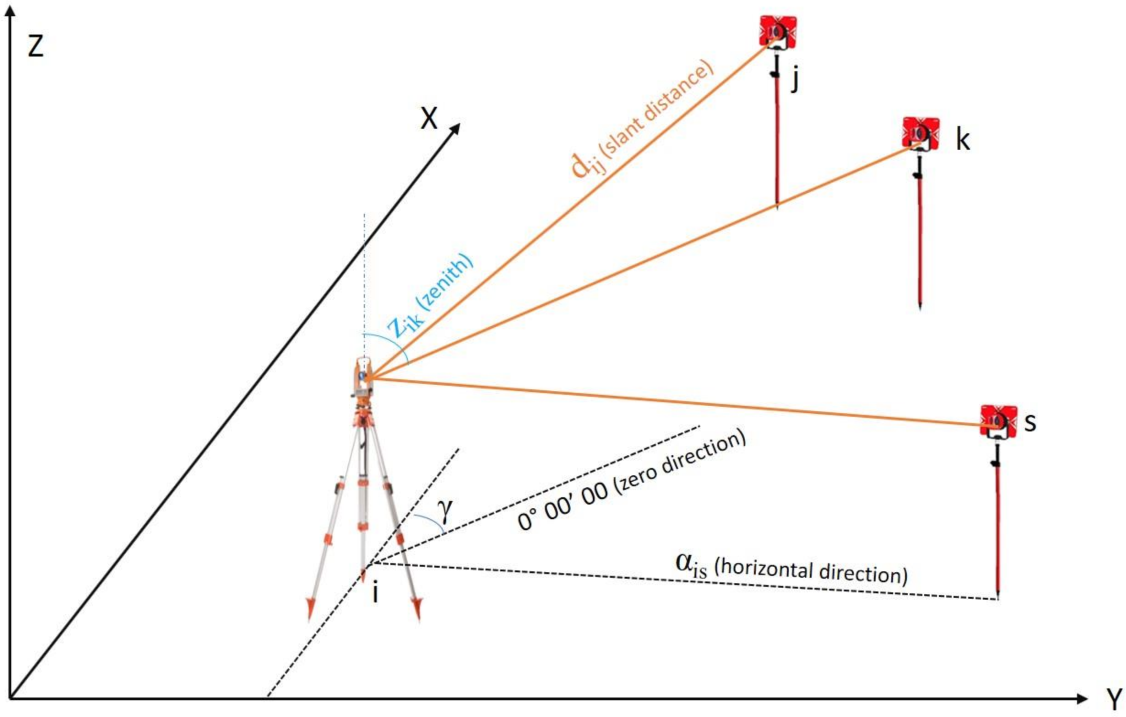

Figure 3. Illustration of 3D triangulation.

The observation equation for the slant distance (d_{ij}), horizontal direction (α_{ij}), and zenith angles (z_{ij}) between point i (e.g. the standing point or total station position) and points j (e.g. the reference markers on the IMU chasing and the reflector or aiding sensor) can be written as follows:

$$d_{ij} + r_{ij}^{d} = \sqrt{\left(\Delta X_{ij}\right)^2 + \left(\Delta Y_{ij}\right)^2 + \left(\Delta Z_{ij}\right)^2} \quad (1)$$

$$\alpha_{ij} + r_{ij}^{\alpha} = atan\left(\frac{\Delta Y_{ij}}{\Delta X_{ij}}\right) + \gamma \quad (2)$$

$$z_{ij} + r_{ij}^{z} = atan\left(\frac{\sqrt{\left(\Delta X_{ij}\right)^2 + \left(\Delta Y_{ij}\right)^2}}{\Delta Z_{ij}}\right) \quad (3)$$

where r_{ij}^{d}, r_{ij}^{α} and r_{ij}^{z} are the residuals associated with observed quantities, $\Delta X_{ij} = X_j - X_i$, $\Delta Y_{ij} = Y_j - Y_i$, $\Delta Z_{ij} = Z_j - Z_i$ are the differences between point coordinates, and γ is the orientation of the zero direction of the instrument with respect to the X-axis direction of IMU. Linearization of the above non-linear functions can be done using Taylor's series expansion expressed in Eq.(4) where $X_i^0, Y_i^0, Z_i^0, X_j^0, Y_j^0, Z_j^0$ and $\delta X_i, \delta Y_i, \delta Z_i, \delta X_j, \delta Y_j, \delta Z_j$ are the approximate values and the correction terms of the unknown coordinates of points i and j, respectively. It should be noted that one more term $\left[\frac{\partial F}{\partial \gamma}\right]^0 \delta\gamma$ is added to the above equation when the horizontal directions are being linearized.

$$F\left(X_i, Y_i, Z_i, X_j, Y_j, Z_j\right) = F\left(X_i^0, Y_i^0, Z_i^0, X_j^0, Y_j^0, Z_j^0\right) + \left[\frac{\partial F}{\partial X_i}\right]^0 \delta X_i + \left[\frac{\partial F}{\partial Y_i}\right]^0 \delta Y_i + \left[\frac{\partial F}{\partial Z_i}\right]^0 \delta Z_i + \left[\frac{\partial F}{\partial X_j}\right]^0 \delta X_j + \left[\frac{\partial F}{\partial Y_j}\right]^0 \delta Y_j + \left[\frac{\partial F}{\partial Z_j}\right]^0 \delta Z_j \quad (4)$$

The corresponding linearized forms of the slant distance, horizontal direction, and zenith angle are given as below by taking the partial derivatives:

$$\Delta d_{ij} + r_{ij}^{d} = \frac{\Delta X_{ij}^0}{d_{ij}^0}\delta X_j + \frac{\Delta Y_{ij}^0}{d_{ij}^0}\delta Y_j + \frac{\Delta Z_{ij}^0}{d_{ij}^0}\delta Z_j - \frac{\Delta X_{ij}^0}{d_{ij}^0}\delta X_i - \frac{\Delta Y_{ij}^0}{d_{ij}^0}\delta Y_i - \frac{\Delta Z_{ij}^0}{d_{ij}^0}\delta Z_i \quad (5)$$

$$\Delta \alpha_{ij} + r_{ij}^{\alpha} = \delta\gamma - \frac{\Delta Y_{ij}^0}{\left(s_{ij}^0\right)^2}\delta X_j + \frac{\Delta X_{ij}^0}{\left(s_{ij}^0\right)^2}\delta Y_j + \frac{\Delta Y_{ij}^0}{\left(s_{ij}^0\right)^2}\delta X_i - \frac{\Delta X_{ij}^0}{\left(s_{ij}^0\right)^2}\delta Y_i \quad (6)$$

$$\Delta z_{ij} + r_{ij}^{z} = \frac{\Delta X_{ij}^{0}}{t_{ij}^{0}}\delta X_j + \frac{\Delta Y_{ij}^{0}}{t_{ij}^{0}}\delta Y_j - \frac{\left(s_{ij}^{0}\right)^2}{k_{ij}^{0}}\delta Z_j - \frac{\Delta X_{ij}^{0}}{t_{ij}^{0}}\delta X_i - \frac{\Delta Y_{ij}^{0}}{t_{ij}^{0}}\delta Y_i + \frac{\left(s_{ij}^{0}\right)^2}{k_{ij}^{0}}\delta Z_i \quad (7)$$

where

$$\Delta X_{ij}^{0} = X_j^0 - X_i^0$$
$$\Delta Y_{ij}^{0} = Y_j^0 - Y_i^0$$
$$\Delta Z_{ij}^{0} = Z_j^0 - Z_i^0$$
$$d_{ij}^{0} = \sqrt{\left(\Delta X_{ij}^{0}\right)^2 + \left(\Delta Y_{ij}^{0}\right)^2 + \left(\Delta Z_{ij}^{0}\right)^2}$$
$$s_{ij}^{0} = \sqrt{\left(\Delta X_{ij}^{0}\right)^2 + \left(\Delta Y_{ij}^{0}\right)^2} \quad (8)$$
$$t_{ij}^{0} = \left(\frac{\left(s_{ij}^{0}\right)^2 + \left(\Delta Z_{ij}^{0}\right)^2}{\Delta Z_{ij}^{0}}\right) s_{ij}^{0}$$
$$k_{ij}^{0} = \left(s_{ij}^{0}\right)^2 + \left(\Delta Z_{ij}^{0}\right)^2$$
$$\Delta d_{ij} = d_{ij} - d_{ij}^{0}$$
$$\Delta \alpha_{ij} = \alpha_{ij} - \alpha_{ij}^{0} = \alpha_{ij} - atan\left(\frac{\Delta Y_{ij}^{0}}{\Delta X_{ij}^{0}}\right) + \gamma^0$$
$$\Delta z_{ij} = z_{ij} - z_{ij}^{0} = z_{ij} - atan\left(\frac{s_{ij}^{0}}{\Delta Z_{ij}^{0}}\right)$$

The matrix form for linearized observation equations in Eqs. (5-7) can be written as follows:

$$\boldsymbol{A}\delta\boldsymbol{x} = \Delta\boldsymbol{c} + \boldsymbol{r} \quad (9)$$

where $\boldsymbol{A}$ is the design matrix constituted of partial derivatives, $\delta\boldsymbol{x} = \left[\delta X_i, \delta Y_i, \delta Z_i, \delta X_j, \delta Y_j, \delta Z_j, \delta\gamma\right]^{\mathrm{T}}$ is the vector of corrections applied to the unknowns, $\Delta\boldsymbol{c} = \left[\Delta d_{ij}, \Delta\alpha_{ij}, \Delta z_{ij}\right]^{\mathrm{T}}$ is the vector of closures, and $\boldsymbol{r}$=$\left[r_{ij}^{d}, r_{ij}^{\alpha}, r_{ij}^{z}\right]^{\mathrm{T}}$ is the vector of residuals. The least squares solution of Eq. (9) is given by:

$$\delta\widehat{\boldsymbol{x}} = (\boldsymbol{A}^{\mathrm{T}}\boldsymbol{A})^{-1}\boldsymbol{A}^{\mathrm{T}}\Delta\boldsymbol{c} \quad (10)$$

If the measurements are uncorrelated but have different uncertainties, then the weight matrix becomes $\boldsymbol{W} = diag\left(1/\left[\boldsymbol{\sigma}_{d_{ij}}^2, \boldsymbol{\sigma}_{\alpha_{ij}}^2, \boldsymbol{\sigma}_{z_{ij}}^2\right]\right)$, and the weighted least squares solution can be written as:

$$\delta\widehat{\boldsymbol{x}} = (\boldsymbol{A}^{\mathrm{T}}\boldsymbol{W}\boldsymbol{A})^{-1}\boldsymbol{A}^{\mathrm{T}}\boldsymbol{W}\Delta\boldsymbol{c} \quad (11)$$

The estimated corrections are added to the approximate values to compute the updated values of the approximations after each iteration. The best estimates are obtained when the corrections for the kth iteration reach some desired value, say less than 0.5 mm.

$$\widehat{\boldsymbol{x}} = \boldsymbol{x}^0 + \delta\widehat{\boldsymbol{x}} = \left[X_i^0, Y_i^0, Z_i^0, X_j^0, Y_j^0, Z_j^0, \gamma^0\right]^{\mathrm{T}} + \left[\delta X_i, \delta Y_i, \delta Z_i, \delta X_j, \delta Y_j, \delta Z_j, \delta\gamma\right]^{\mathrm{T}} \quad (12)$$

At the end of the iterative process, the residuals are computed from Eq. (9) and the quality of the observations is assessed. Large residuals may indicate poor observations and should be removed or remeasured.

3. DESIGN AND IMPLEMENTATION

An experimental setup has been designed in laboratory conditions using an IMU and total station reflector shown in Figure 4 to allow direct measurement of the true or exact aiding sensor lever arm vector for accuracy assessment. The IMU is the navigation-grade iNAT-RQH of iMAR Navigation GmbH (https://www.imar-navigation.de/). It has some reference markers on its casing (see Figure 5) that can easily be measured with a caliper or a ruler. The company provides the mechanical drawings of the system which depict the locations of the sensor intersection point (the origin of the inertial sensor coordinate frame) and the reference markers. The sensor intersection point is the point somewhere inside the IMU not visible from outside. The provided drawings display the precise offset values between the sensor intersection point and the front left corner of the IMU which enables us to make the appropriate transformation after the successful determination of the aiding sensor lever arm with respect to the front left corner. For our case, the offset values between these two points are [0.1210, -0.1275, 0.1160] meters in X, Y, and Z directions, respectively.

The reflector on the top of the IMU represents the aiding sensor. The verticality of the reflector has been ensured by the total station. The 3D position of the reflector with respect to the front left corner of the IMU has been precisely measured by cross-checking with different instrumentations such as a ruler, caliper, laser meter, and tape measure. The obtained values [-0.125, 0.066, -1.554] meters in X, Y, and Z directions are acknowledged as the true coordinates of the aiding sensor.

Topcon OS-103 total station, having angle measurement accuracy of 3" and distance measurement accuracy of about (3 + 2ppm x D) mm where D is the measuring distance in mm, is setup approximately 10 meters away from the reflector with the best visibility to all reference points. It should be noted that the total station should be placed as close as possible to the IMU chasing in practical application, but great care should be exercised in order not to obstruct the visibility to the reference markers and the aiding sensor.

Figure 4. Experimental setup with IMU, reflector, and total station.

Figure 5. The iCORUS reference points (markers) given in Table 1 and coordinate axis directions on the top of the IMU.

More information about the specifications of Topcon OS-103 can be found in the product sheet at https://www.topcon.co.jp/en/positioning/products/pdf/OS_E.pdf. The instrument is carefully levelled and the zero direction is oriented approximately towards the X-axis direction of the IMU to initialize the approximate value of γ with zero. Slant distances, horizontal directions, and the zenith angles to the reference points and the reflector are measured subsequently. The exact coordinates of the reference points on the IMU chasing and the initial coordinates of the standing point and the reflector are presented in Table 1, the observations are listed in Table 2, and the measurement uncertainties and their corresponding weights are given in Table 3.

Table 1: The list of the exact and approximate coordinates of the reference (from L-F to T-2) and unknown points (reflector and standing) in the inertial sensor coordinate frame.

Point Name	X [cm]	Y [cm]	Z [cm]
L-F	0.00	0.00	0.00
L-1	-2.73	0.25	-1.30
L-2	-2.73	0.25	-9.30
L-3	-2.73	0.25	-17.30
L-4	-4.73	0.25	-0.50
L-5	-4.73	0.25	-18.20
L-6	-14.23	0.25	-0.50
L-7	-14.23	0.25	-18.20
L-8	-23.73	0.25	-0.50
L-9	-23.73	0.25	-18.20
L-10	-33.23	0.25	-0.50
L-11	-33.23	0.25	-1.30
L-12	-35.23	0.25	-1.30
L-13	-35.23	0.25	-9.30
L-14	-35.23	0.25	-17.30
L-B	-38.00	0.00	0.00
T-1	-9.55	4.85	-20.20
T-2	-18.55	4.85	-20.20
Reflector (GNSS Antenna)	-12.40	3.86	-140.00
Standing (Total Station)	-36.50	-1085.00	-120.50

4. RESULTS AND CONCLUSION

A MATLAB function attached in the appendix has been written to perform 3D triangulation described in section 2. In our case with a single GNSS antenna, there are 7 unknowns (e.g. u=7), 57 observations (e.g. n=57), and 18 reference points that possess fixed coordinates to solve the problem. The unknows are the 3D coordinates of the reflector (X_G, Y_G, Z_G) and the standing point

(X_T, Y_T, Z_T), and also the 1D orientation of the zero direction of the total station (γ) with respect to the X-axis direction of IMU. "lscov.m" function of MATLAB for weighted least squares solution to the linear system is used to evaluate Eq. (11). A while loop is employed for the iterative solution. The design matrix $\boldsymbol{A}$ and the closure vector $\Delta\boldsymbol{c}$ are rebuilt with the most recent values of the unknowns. The iteration is terminated when all the corrections $\delta\boldsymbol{x}$ applied to the unknown coordinates are less than 0.5 mm. The best estimate of the reflector coordinates in the inertial sensor coordinate frame after two iterations are presented in Table 4. It is evident that the deviations of the estimates from the true values are less than 0.5 cm.

Table 2: The slant distance, horizontal direction, and zenith angle measurements from standing (Total Station) to all visible points.

Point Name	Slant Distance [m]	Horizontal Direction [degree]	Zenith Angle [degree]
L-F	10.851	89.336667	96.310000
L-1	10.853	89.483611	96.238056
L-2	10.847	89.479167	95.818333
L-3	10.844	89.474444	95.396667
L-4	10.852	89.588889	96.282222
L-5	10.845	89.582222	95.352222
L-6	10.853	90.095000	96.278333
L-7	10.839	90.086389	95.351389
L-8	10.851	90.597222	96.275833
L-9	10.838	90.588611	95.347222
L-10	10.843	91.103889	96.271111
L-11	10.838	91.096111	95.343611
L-12	10.843	91.208333	96.227500
L-13	10.842	91.206667	95.806667
L-14	10.838	91.201945	95.384167
L-B	10.841	91.362778	96.299722
T-1	10.873	89.869722	95.248889
T-2	10.872	90.346111	95.242500
Reflector	10.866	90.023056	87.895000

Table 3: Measurement uncertainties and corresponding weights.

Measurement	Uncertainty	Weight
Slant distance	3 mm	0.3333 mm^{-1}
Angular meas.	3"	9.26E-5 rad^{-1}

Table 4: True and best estimate values of the reflector coordinates.

	X [m]	Y [m]	Z [m]
True value	-0.125	0.066	-1.554
Best estimate	-0.127	0.070	-1.551

Today's kinematic GNSS accuracies for the horizontal and vertical coordinate components are about few centimeters or even worse in some cases. The experimental results reveal that the GNSS antenna lever arm can accurately be determined via 3D triangulation technique using a medium quality total station. It is hoped that the study and the MATLAB function attached will help the non-geodesists working in the inertial navigation field, particularly the novice researchers wondering about the accurate determination of the lever arm vector by triangulation. It should be noted that the methodology can also be applied for the lever arm determination of the different aiding sensors used in inertial navigation.

APPENDIX

The MATLAB function named "LeverArm3DTri.m" that can perform 3D triangulation and the paper itself are combined into a single zipped folder downloadable from the journal's web site at https://www.harita.gov.tr/makaleler. It can also be attained from the ResearchGate page of the first author.

ORCID

Mehmet SİMAV https://orcid.org/0000-0002-3963-3871

Yunus Aytaç AKDOĞAN https://orcid.org/0000-0003-2232-5327

REFERENCES

Alsadik, B. (2019). *Adjustment models in 3D geomatics and computational geophysics with MATLAB examples*. Elsevier, Amsterdam.

Awange, J.L. and Grafarend, E.W. (2005). *Solving algebraic computational problems in geodesy and geoinformatics*. Springer, Berlin.

Bell, T. (2000). Error analysis of attitude measurement in robotic ground vehicle position determination. *Navigation*, *47*(4), 289-296. doi: 10.1002/j.2161-4296.2000.tb00222.x

Borko, A., Klein, I. and Even-Tzur, G. (2018). GNSS/INS fusion with virtual lever-arm measurements. *Sensors*, *18*(7), 2228. doi: 10.3390/s18072228

Farrell, J.A. (2008). *Aided navigation: GPS with high rate sensors*. McGraw-Hill, New York

Grewal, M.S., Andrews, A.P. and Bartone, C.G. (2013). *Global navigation satellite systems, inertial navigation and integration*. John Wiley & Sons.

Groves, P.D. (2013). *Principles of GNSS, inertial, and multisensor integrated navigation systems*. Artech House: Norwood, MA.

He, X. and Jianye, L. (2002). Analysis of lever arm effects in GPS/IMU integration system. *Trans. Nanjing Univ. Aeronaut. Astronaut*, *19*(1), 59-64.

Hong, S., Chang, Y-S., Ha, S-K. and Lee, M-H. (2002). Estimation of alignment errors in GPS/INS integration. *Proceedings of the 15th International Technical Meeting of the Satellite Division of The Institute of Navigation (ION GPS 2002)*, Portland, OR, pp 527-534.

Hong, S., Lee, M-H., Kwon, S-H. and Chun, H-H. (2004). A car test for the estimation of GPS/INS alignment errors. *IEEE Transactions on Intelligent Transportation Systems*, *5*(3), 208-218. doi: 10.1109/TITS.2004.833771

Hong, S., Lee, M-H., Chun, H-H., Kwon, S-H. and Speyer, J.L. (2005). Observability of error states in GPS/INS integration. *IEEE Transactions on Vehicular Technology, 54*(2), 731-743. doi: 10.1109/TVT.2004.841540

Hong, S., Lee, M-H., Chun, H-H., Kwon, S-H. and Speyer, J.L. (2006). Experimental study on the estimation of lever arm in GPS/INS. *IEEE Transactions on Vehicular Technology*, *55*(2), 431-448. doi: 10.1109/TVT.2005.863411

Jekeli, C. (2001). *Inertial navigation systems with geodetic applications*. Walter de Gruyter, Berlin.

Lee, M.K., Hong, S., Lee, M-H., Kwon, S-H. and Chun, H-H. (2005). Observability analysis of alignment errors in GPS/INS. *Journal of Mechanical Science and Technology, 19*(6), 1253-1267. doi: 10.1007/BF02984046

Luhmann, T., Robson, S., Kyle, S. and Boehm, J. (2020). *Close-range photogrammetry and 3D imaging*. Walter de Gruyter, Berlin.

Montalbano, N. and Humphreys, T. (2018). A comparison of methods for online lever arm estimation in GPS/INS integration. *IEEE/ION Position, Location and Navigation Symposium (PLANS)*, pp 680-687. doi: 10.1109/PLANS.2018.8373443

Ogundare, J.O. (2019). *Understanding least squares estimation and geomatics data analysis*. John Wiley & Sons, Hoboken.

Seo, J., Lee, H-K., Lee, J.G. and Park, C.G. (2006). Lever arm compensation for GPS/INS/odometer integrated system. *Int. J. Control Autom. Syst.,4*(2), 247-254.

Stovner, B.N. and Johansen, T.A. (2019). GNSS-antenna lever arm compensation in aided inertial navigation of UAVs. *18th European Control Conference (ECC)*. doi: 10.23919/ECC.2019.8795760

Titterton, D.H. and Weston, J.L. (2004). *Strapdown inertial navigation technology*. IET, Stevenage.

Torge, W. (2001) *Geodesy*. Walter de Gruyter, Berlin.

Wu, Y., Wang, J. and Hu, D. (2014). A new technique for INS/GNSS attitude and parameter estimation using online optimization. *IEEE Transactions on Signal Processing*, *62*(10), 2642-2655. doi: 10.1109/TSP.2014.2312317